

## Sb doping of Si molecular-beam epitaxial layers: Influence of the substrate misorientation

M. Ladevèze, F. Bassani, F. Arnaud d'Avitaya, and G. Tréglià

CRMC2, Centre National de la Recherche Scientifique, Campus de Luminy, Case 913, 13288 Marseille Cedex 9, France

C. Dubois

LPM-CNRS, INSA, Bât. 502, 20 av. A. Einstein, 69621 Villeurbanne Cedex, France

R. Stuck

Laboratoire Phase-CNRS, Boîte Postale 20, 67037 Strasbourg Cedex 2, France

(Received 14 March 1997)

The influence of the misorientation of the surface on the doping of Si(111) by Sb under codeposition in a molecular-beam epitaxy chamber is experimentally evidenced by secondary ion mass spectrometry measurements. The Sb incorporation presents the same qualitative behavior (it is almost constant down to a critical temperature, below which it abruptly increases) for flat and misoriented substrates, but with a shift towards lower temperature in the latter case. This can be understood in terms of local equilibrium, as the result of the coupling between desorption and segregation phenomena during the incorporation process. The difference between the nominal and vicinal substrates is then ascribed to the existence of a temperature range [700 °C–780 °C] for which desorption essentially concerns Sb atoms adsorbed on step sites. [S0163-1829(97)04836-4]

### I. INTRODUCTION

Molecular-beam epitaxy of silicon (MBE-Si) is a useful tool both from the fundamental and applied points of view.<sup>1</sup> Among other applications, this technique is used for fabricating hyperfrequency diodes (IMPATT) for which control of the doping profile is a determining quality factor.<sup>2</sup> In most cases, the growth is performed on flat (111) or (100) surfaces. However, in order to favor a step flow (instead of three-dimensional) growth mode, one can be tempted to introduce steps on the surface, which requires the use of misoriented substrates. Unfortunately, existing knowledge regarding dopant incorporation acquired on *flat* surfaces does little to alleviate the need for similar knowledge applied to *stepped* surfaces since steps markedly affect dopant incorporation and consequently doping profiles. Our aim here is to illustrate this influence in the case of the antimony (Sb)-doped Si(111) system, for which preliminary studies of misoriented substrates have already been performed concerning both the homoepitaxy<sup>3</sup> and the dopant adsorption.<sup>4</sup> We will show that the differences between the doping profiles obtained for nominal and vicinal surfaces can be fully understood in light of the latter studies.

### II. SURVEY OF THE EXISTING SITUATION

From the experimental point of view, among the possible *N*-type doping elements of Si, Sb is probably the most widely used in the field of MBE. This is due to its rather low vapor pressure (compared to As or P) which allows it to be evaporated from a standard effusion cell. Usually it is codeposited with Si on the Si substrate, using two distinct sources in order to better control the ratio of the two fluxes and then the doping level. Unfortunately, the *actual* doping level seldom corresponds to the *ideal* one defined as this flux ratio.

Indeed, previous experiments performed on nominal substrates have shown that, depending on the substrate temperature, the incorporation can be incomplete, the maximum doping level being found lower than the solubility limit. This has been interpreted as due to a strong segregation of Sb at the surface, leading to a surface layer acting as a reservoir from which Sb atoms can be incorporated.<sup>5,6</sup> More precisely, by plotting the experimental temperature dependence of the incorporation coefficient (defined as the ratio between the *actual* doping and the *ideal* one) Metzger and Allen<sup>7</sup> have put in evidence the existence of two distinct temperature regimes: one above 700 °C where *equilibrium* segregation can be achieved (leading to an Arrhenius behavior) and the other below 700 °C where segregation is *kinetically* limited. Moreover, they were also able to show that both desorption and incorporation were first order processes. In order to get a more precise idea of the influence of surface segregation, it was then interesting to determine the variation of the doping with surface coverage at a given temperature. This was experimentally performed by Delage *et al.*,<sup>8</sup> in the high temperature regime (at 760 °C), who found that the increase of doping with increasing coverage was far from being linear but that, at this temperature, it could be considered as following the surface segregation isotherm (exponential type shape).

From the theoretical point of view, several models have been developed in order to understand the temperature dependence of the Sb doping profile on nominal Si substrates by MBE. Using phenomenological flux equations, and assuming that doping is proportional to the surface coverage, Iyer *et al.*<sup>9</sup> were able to reproduce the experimental high temperature (Arrhenius type) behavior of the incorporation coefficient but not the one at lower temperature. This failure could be due to their assumption that doping was proportional to surface coverage which, as previously mentioned,

was experimentally denied, even above 700 °C,<sup>8</sup> due to strong surface segregation. It was then essential for models to account properly for the actual segregation isotherm, which was done in the following works of Barnett and Green<sup>10</sup> who used a continuous model for codeposition, and of Jorke<sup>11</sup> who treated in a discrete way Si deposition on a Si surface initially covered by Sb. These authors were then able to fit the experimental behavior of the incorporation coefficient on the whole temperature range [600 °C–900 °C].

However, it is worth pointing out that all these studies only concerned the doping of nominal surfaces but that, at least to our knowledge, none has concerned vicinal ones, and the influence of miscut, up to now. This is what we aim to do in the following, both from the experimental and theoretical points of view.

### III. EXPERIMENTAL SETUP

Sb-doped epitaxial Si layers were grown in a MBE apparatus using an electron beam evaporator for Si and a standard RIBER temperature controlled effusion cell for coevaporation of Sb. The Sb flux was varied in the [ $10^{12}$ – $10^{14}$ ] at/(cm<sup>2</sup> s) range, calibrated from Rutherford backscattering measurements, by regulating the cell temperature between 350 °C and 450 °C. The Si substrates were either nominal Si(111) crystals or vicinal ones, presenting different misorientations (2°, 6°, and 10°) around [1–10] towards [–1–12]. The surfaces were cleaned first chemically *ex situ* and then thermally *in situ*. After this treatment, the nominal surface exhibited a clear (7×7) low energy electron diffraction (LEED) pattern. Moreover it developed very large terraces (100–200 nm) limited by single-height steps. The situation was found very different for the misoriented surface. Indeed, in that case the LEED spots were splitted, indicating a regular array of steps. For the 10° misorientation this array exhibited a 5.3 nm periodicity, which allowed us<sup>3</sup> to conclude that these steps were triple-height, with terrace widths of 2.3 nm and step edge widths of 3 nm. Codeposition of Sb and Si was then performed on these substrates. In order to study the temperature dependence of Sb doping, we performed two series of experiments in two different temperature regimes: a high one (700 °C <  $T$  < 775 °C) and a low one (625 °C <  $T$  < 700 °C). Each series was performed by using the same sample on which four thick (~300 nm) Sb-doped films were deposited, each one with a different substrate temperature. The growth rate was  $V_g = 0.15$  nm/s and the Si and Sb fluxes were kept constant for the four films. The typical growth pressure during deposition was  $10^{-10}$  mbar. The Sb concentration depth profiles were then measured by secondary ion mass spectrometry. It is worth noticing that, in order to get a meaningful comparison between the dopant incorporation on both surfaces, it was essential to perform the measurements with identical conditions to avoid differences due to variations in the growth rate, the incident Sb flux ( $F_{Sb}$ ), and the substrate temperature ( $T$ ). To this aim, we have elaborated a sample holder which could support two samples (a nominal and a vicinal one) with symmetrical positions, allowing the deposit of Sb and Si on both surfaces simultaneously. Thus, even though temperature was not uniform for each sample surface, it was for the two samples. The results which are shown in the

following section have then been measured for symmetrical points (except in one particular case which will be detailed).

### IV. EXPERIMENTAL RESULTS

Let us first comment on the variation of the Sb incorporation with temperature for a nominal Si(111) surface and a vicinal one in the high temperature regime. One can see in Figs. 1(a) and 1(d) the doping profiles obtained for two symmetrical points (on the sample holder), corresponding, respectively, to a nominal substrate [Fig. 1(a)] and a 10° mis-oriented one [Fig. 1(d)]. In this series, the Sb flux was  $F_{Sb} = 10^{14}$  at/(cm<sup>2</sup> s). The first film was prepared at  $T = 700$  °C, and then the temperature was increased by 25 °C steps for the following films. Each different film appears in the figures as a plateau, under the indication of the corresponding temperature. The most striking feature is that for the nominal sample, the doping remains constant when the temperature is decreased, at least down to a *critical* value ( $T \sim 750$  °C), below which suddenly it steeply increases. A similar behavior is observed for the vicinal surface but with a lower *critical* temperature ( $T \sim 700$  °C).

The doping profiles in the low temperature regime are exhibited in Fig. 2(a) (for the nominal surface) and Fig. 2(b) (for the vicinal one). It is worth noting that, in this series, we have lowered the Sb flux to  $F_{Sb} = 10^{12}$  at/(cm<sup>2</sup> s), in order not to reach the solubility limit ( $2 \times 10^{19}$  at/cm<sup>3</sup> at 600 °C) as a consequence of the increase of the incorporation when temperature decreases. Contrary to what we have done in the high temperature regime, we deposited the first film at the highest temperature ( $T = 675$  °C) and then decreased the temperature by 25 °C steps for the following ones, in order to optimize the crystalline quality of the substrate. Indeed, starting from the lowest temperature would have given us a first substrate with a poor crystalline quality, which should be inherited by the following films. The comparison between Fig. 2(a) and Fig. 2(b) reveals a slightly lower doping level for the misoriented sample, but which is not sufficiently significant to be sure that it is not due to imperfect symmetry between the measurement points. Indeed, we will see in the following that doping is extremely temperature dependent in this temperature range. Then, the main conclusion that one can draw is that, contrary to what was observed in the high temperature regime, the temperature dependence of doping is identical for both substrates in the low temperature regime.

Finally, one can note a difference between the two temperature regimes concerning the transient states between each film. Indeed, such transient states are clearly seen in the low temperature series (Fig. 2), as a doping decrease after the growth of each film, whereas they are not in the high temperature regime (Fig. 1). This is due to our procedure in which, between each deposit, we have evaporated the surface Sb layer to avoid any *memory effect* for the following deposit, but in a more efficient way in the former than in the latter case.

To summarize, one can say that the doping profile presents the same trend as a function of temperature for both substrates. Namely, it is constant down to a *critical* temperature  $T_c$  below which it increases abruptly. The only difference between the two orientations is that the value of  $T_c$  is larger for the nominal than for the misoriented substrate. To

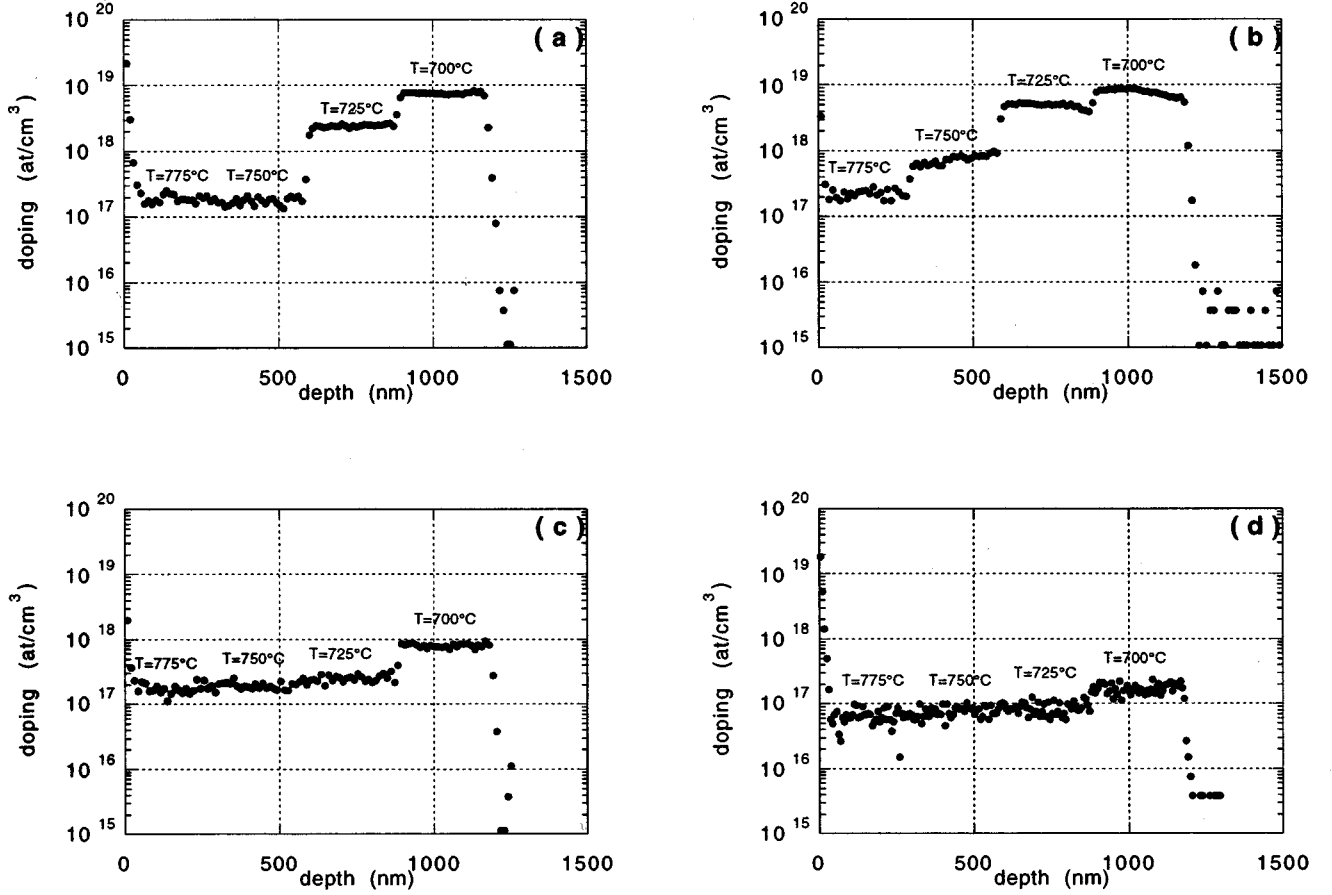


FIG. 1. Temperature dependence of the doping profile in the high temperature and Sb flux ( $T, F_{\text{Sb}}$ ) regime [ $T > 700^\circ\text{C}$  and  $F_{\text{Sb}} = 10^{14}$  at/( $\text{cm}^2 \text{s}$ )], as a function of the misorientation angle  $\alpha$ . (a):  $\alpha = 0^\circ$ ; (b):  $\alpha = 2^\circ$ ; (c):  $\alpha = 6^\circ$ ; (d):  $\alpha = 10^\circ$ .

confirm this homothetical behavior, it would be interesting to extend the doping profiles found for the misoriented surface [Fig. 1(d)], with the same flux [ $F_{\text{Sb}} = 10^{14}$  at/( $\text{cm}^2 \text{s}$ )], on its lower temperature side. This can be done in a somewhat approximate way by adding to the previous data [Fig. 1(d)], measured in the center of the sample, those that we obtained by measuring the same profiles near the edge of the sample, for which the temperature is lower by about  $50^\circ\text{C}$ . This allows us to add two films to the four previous ones, as illustrated in Fig. 3. As can be seen by comparing Fig. 1(a) and Fig. 3, the behavior for the misoriented surface is indeed the same as for the nominal one, with a temperature shift of about  $50^\circ\text{C}$ . Finally, it is worth noting that varying the misorientation angle between the two used before ( $0^\circ$  and  $10^\circ$ ) leads to intermediate observations which are consistent with the previous ones, at least in the limits of what could be expected from a set of experiments performed in not completely identical conditions. This overall consistency is illustrated, in the high flux and temperature regime, in Fig. 1(b) and Fig. 1(c). Indeed, the behavior observed for a  $2^\circ$  misorientation is found very similar to the one obtained for the nominal surface whereas that observed for the  $6^\circ$  one looks like that obtained for the  $10^\circ$  misorientation. Nevertheless the accuracy is not sufficient to determine if the behavior varies continuously as a function of the miscut angle or if there exists some critical angle in between.

## V. MODEL

A full treatment of doping requires to include in a same model all the driving forces of the phenomena, which bring into play the balance between the various fluxes, respectively, due to deposition (incoming flux:  $F_{\text{Sb}}$ ), desorption ( $J_{\text{des}}^{\text{Sb}}$ ), and incorporation ( $J_{\text{inc}}^{\text{Sb}}$ ). Let us denote  $c_p$  the Sb concentration in the  $p$  plane parallel to the surface (labeled  $p = 0$ ):  $c_p = N_p^{\text{Sb}}/N_p$ , where  $N_p^{\text{Sb}}$  is the number of Sb atoms in the  $p$  plane and  $N_p$  the number of sites in this plane. Except for  $p = 0$ ,  $N_p = N$ , i.e., the number of sites of a close-packed Si(111) layer. The time dependence of  $N_0$  is driven by the Si flux. In this framework, the variation of the Sb concentrations at the surface ( $p = 0$ : surface coverage) and in the planes below ( $p > 1$ ) is given by

$$\frac{\partial c_0}{\partial t} = F_{\text{Sb}} - J_{\text{des}}^{\text{Sb}} - J_{0 \rightarrow 1}^{\text{Sb}}, \quad (1)$$

$$\frac{\partial c_{p>0}}{\partial t} = J_{p-1 \rightarrow p}^{\text{Sb}} - J_{p \rightarrow p+1}^{\text{Sb}}, \quad (2)$$

where  $J_{p \rightarrow q}^{\text{Sb}}$  is the Sb net flux from the  $p$  layer to the  $q$  layer ( $q = p \pm 1$ ):

$$J_{p \rightarrow q}^{\text{Sb}} = c_p(1 - c_q)\Gamma_{p \rightarrow q}^{\text{Sb}} - c_q(1 - c_p)\Gamma_{q \rightarrow p}^{\text{Sb}} \quad (3)$$

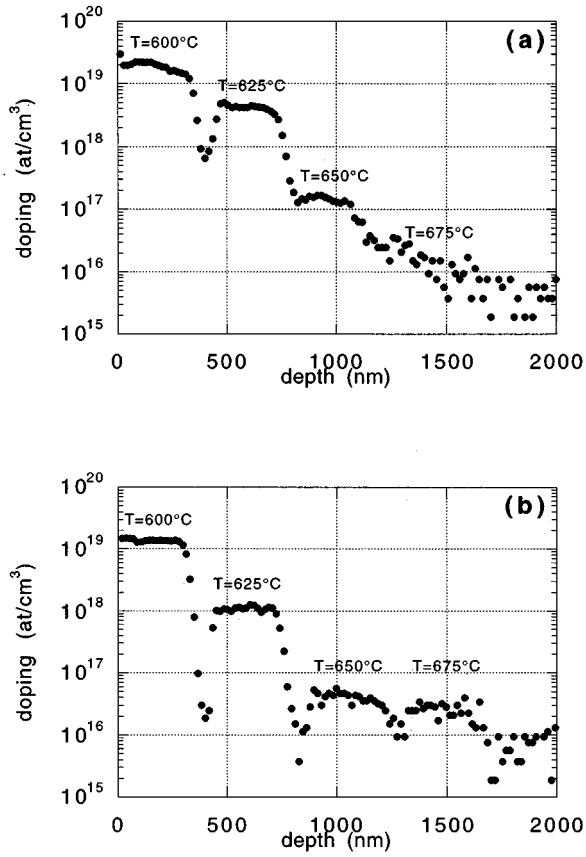


FIG. 2. Temperature dependence of the doping profile in the low ( $T, F_{\text{Sb}}$ ) regime [ $T < 700^\circ\text{C}$  and  $F_{\text{Sb}} = 10^{12}$  at/(cm<sup>2</sup> s)], as a function of the misorientation angle  $\alpha$ . (a):  $\alpha = 0^\circ$ ; (b):  $\alpha = 10^\circ$ .

in which  $\Gamma_{p \rightarrow q}^{\text{Sb}}$  is the exchange frequency of a Sb atom in the  $p$  layer with a Si atom in the  $q$  layer. The incorporation flux, which comes from the balance between the flux of Sb atoms diffusing from the surface to the first underlayer and that of atoms of the first underlayer attracted to the surface by segregation driving forces, can then be written:

$$J_{\text{inc}}^{\text{Sb}} = J_{0 \rightarrow 1}^{\text{Sb}}. \quad (4)$$

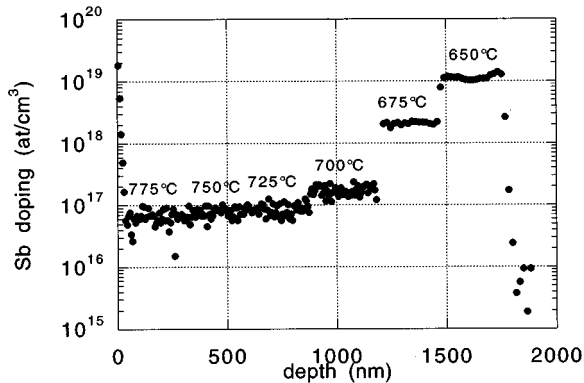


FIG. 3. Temperature dependence of the doping profile for the  $10^\circ$  misoriented surface, extending on a wide temperature range ( $775^\circ\text{C} > T > 650^\circ\text{C}$ ) for a same high value of the Sb flux [ $F_{\text{Sb}} = 10^{14}$  at/(cm<sup>2</sup> s)]. The four high temperature measurements are collected in the middle of the sample (Fig. 1) and the two low ones on the edge.

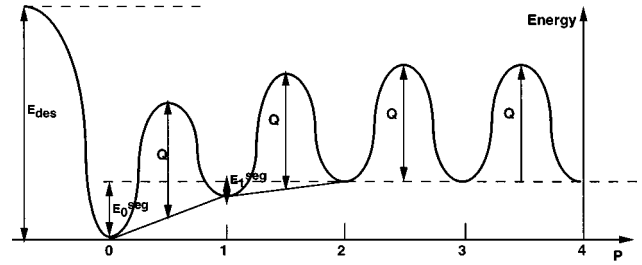


FIG. 4. Activation energy barriers involved in the KTBM model.

On the other hand if one assumes, following Metzger and Allen,<sup>7</sup> that the desorption is of first order, the desorption flux is

$$J_{\text{des}}^{\text{Sb}} = K_{\text{des}} c_0 \quad \text{with} \quad K_{\text{des}} = K_{\text{des}}^0 \exp\left(-\frac{E_{\text{des}}}{kT}\right). \quad (5)$$

The problem is then to determine these exchange frequencies. The least we can do is to ensure that, in absence of incoming and desorbing fluxes, the steady state of the system (1) and (2) corresponds to the equilibrium surface segregation equations for the Si(Sb) system, namely:

$$\frac{c_p}{1 - c_p} = \frac{c_{p+1}}{1 - c_{p+1}} \exp\left\{\frac{E_{p+1}^{\text{seg}} - E_p^{\text{seg}}}{kT}\right\}, \quad (6)$$

where  $E_p^{\text{seg}}$  is the segregation energy in the  $p$  layer, defined as the energy involved when exchanging a Sb atom in a bulk plane with a Si atom in the  $p$  plane. It has been shown from electronic structure calculations<sup>12</sup> that this term is essentially important in the surface plane, in which case  $E_p^{\text{seg}}$  splits into three contributions due to the difference in surface tension and atomic size between the two components and to their tendency to order or phase separate in the bulk alloy. More precisely the first term leads to segregation of the element with the lowest surface tension, the second one to that of the minority atom when it has the largest size, and the third one to that of the minority atom when the bulk alloy presents a tendency to phase separation. In the present case, all the three factors play in favor of Sb surface segregation which is then expected to be strong. Recovering Eq. (6) as the steady state of Eqs. (1) and (2) requires for the frequencies to satisfy the equation:

$$\frac{\Gamma_{p+1 \rightarrow p}^{\text{Sb}}}{\Gamma_{p \rightarrow p+1}^{\text{Sb}}} = \exp\left\{\frac{E_{p+1}^{\text{seg}} - E_p^{\text{seg}}}{kT}\right\}, \quad (7)$$

which allows yet a wide variety of choices. In fact, if one notes  $Q$  the activation energy for diffusion in homogeneous bulk, it has been shown recently (kinetic tight-binding model<sup>13</sup>) that the most realistic choice leads to the activation energy profile schematically illustrated in Fig. 4:

$$\begin{aligned} \Gamma_{p \rightarrow p+1}^{\text{Sb}} &= Z' \nu \exp\left\{-\frac{2Q + E_{p+1}^{\text{seg}} - E_p^{\text{seg}}}{2kT}\right\}; \\ \Gamma_{p+1 \rightarrow p}^{\text{Sb}} &= Z' \nu \exp\left\{-\frac{2Q - E_{p+1}^{\text{seg}} + E_p^{\text{seg}}}{2kT}\right\}, \end{aligned} \quad (8)$$

where  $Z'$  is the number of bonds between two adjacent planes and  $\nu$  a typical phonon frequency.

During the growth, the structure is modified due to the increase of the roughness and to the existence of islands and vacancies. This lowers the potential barrier  $Q$  between the surface plane and the first underlayer, and enhances the surface segregation (step induced segregation). The value of  $Q$  is of a few eV for Sb diffusion in Si bulk so that, at our experimental temperatures, the kinetic barrier is very large which forbids any bulk diffusion. Therefore, the model that we use only concerns the first two layers: the growing surface ( $p=0$ ) and the first underlayer ( $p=1$ ), the remaining crystal being considered as frozen ( $c_2=c_3=\dots=c_b$  where  $c_b$  is the doping level). If one assumes that the segregation energy is only important in the surface plane ( $E_p^{\text{seg}} \neq 0$  for  $p=0$  only), one then finds for  $p=0$ ,

$$\Gamma_{0 \rightarrow 1}^{\text{Sb}} = Z' \nu \exp\left\{-\frac{2Q - E_0^{\text{seg}}}{2kT}\right\};$$

$$\Gamma_{1 \rightarrow 0}^{\text{Sb}} = Z' \nu \exp\left\{-\frac{2Q + E_0^{\text{seg}}}{2kT}\right\}, \quad (9)$$

and for  $p > 0$ ,

$$\Gamma_{p \rightarrow p+1}^{\text{Sb}} = Z' \nu \exp\left\{-\frac{Q}{kT}\right\} = \Gamma_{p+1 \rightarrow p}^{\text{Sb}} = D_{\text{bulk}}, \quad (10)$$

where  $D_{\text{bulk}}$  is the bulk diffusion coefficient. Therefore, all the fluxes vanish except for those between the surface and first underlayer ( $p > 0$ :  $J_{p \rightarrow p+1}^{\text{Sb}} = 0$ ) so that the incorporation flux reduces to

$$J_{\text{inc}}^{\text{Sb}} = J_{0 \rightarrow 1}^{\text{Sb}} = c_0(1 - c_1)\Gamma_{0 \rightarrow 1}^{\text{Sb}} - c_1(1 - c_0)\Gamma_{1 \rightarrow 0}^{\text{Sb}}, \quad (11)$$

and that the system (1) and (2) reduces to two equations to determine  $c_0$  and  $c_1$ :

$$\frac{\partial c_0}{\partial t} = F_{\text{Sb}} - c_0\{K_{\text{des}} + (1 - c_1)\Gamma_{0 \rightarrow 1}^{\text{Sb}}\} + c_1(1 - c_0)\Gamma_{1 \rightarrow 0}^{\text{Sb}}, \quad (12)$$

$$\frac{\partial c_1}{\partial t} = c_0(1 - c_1)\Gamma_{0 \rightarrow 1}^{\text{Sb}} - c_1(1 - c_0)\Gamma_{1 \rightarrow 0}^{\text{Sb}}, \quad (13)$$

since  $(\partial c_{p>1}/\partial t) = 0$ .

Therefore two regimes can occur:

(i) *A kinetic regime*: when the temperature is too low or the growth rate too high, the exchanges at the surface do not have sufficient time to proceed before the incoming of the following layer, so that thermodynamic equilibrium cannot be achieved. In that case, the composition profile is driven by the kinetic equations (12)–(13), in which, for each layer, one has just to take into account exchanges between the growing layer and the one below.

(ii) *A thermodynamical regime*: in the contrary case, i.e., for sufficiently high temperature or slow growth rate, the surface exchange frequencies are large compared to the growth rate and the thermodynamical equilibrium is reached between the two surface layers. One can speak of a *local*

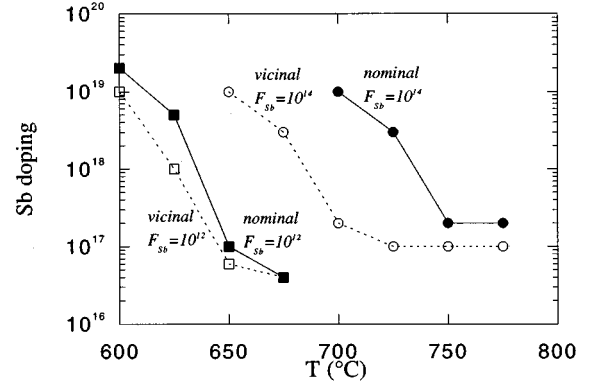


FIG. 5. Temperature dependence of the experimental Sb doping level for the nominal and vicinal ( $10^\circ$  misoriented) surfaces for the two  $(T, F_{\text{Sb}})$  regimes displayed in Figs. 1(a)–1(d) (high) and Fig. 2 (low). Additional data of Fig. 3 are also included.

*equilibrium*.<sup>14</sup> Therefore, the composition profile is determined by the equilibrium equation applied at the surface for the growth of each layer:

$$\frac{c_0}{1 - c_0} = \frac{c_b}{1 - c_b} \exp\left\{-\frac{\Delta E_0^{\text{seg}}}{kT}\right\}, \quad (14)$$

where  $c_b$  is the Sb bulk concentration, i.e., the doping level.

Such a regime of *surface equilibrium* has already been encountered, for instance, in the case of In segregation during growth of  $\text{Ga}_x\text{In}_{1-x}\text{As}/\text{GaAs}$  heterojunctions.<sup>15,16</sup>

## VI. APPLICATION TO THE STUDY OF THE INTERFACE (Si–Sb)/Si

The main experimental results of the Sec. III are collected in Fig. 5, where we plot the variation of the doping level for both nominal and vicinal ( $10^\circ$  misoriented) substrates as a function of temperature, for the two regimes under study which correspond, respectively, to high [Fig. 1(a), Fig. 3] and low (Fig. 2) temperature and Sb flux conditions  $(T, F_{\text{Sb}})$ . The essential features appear in this figure, as follows.

(i) In the high  $(T, F_{\text{Sb}})$  regime, the doping level is constant above  $T_c$  and then sharply increases below, the value of  $T_c$  being lower by about  $50^\circ\text{C}$  for the vicinal surface.

(ii) In the low  $(T, F_{\text{Sb}})$  regime, the doping level increases monotonously with decreasing temperature, in a similar way for both orientations.

(iii) When different fluxes have been used for a given temperature, which is the case for the misoriented surface at  $650^\circ\text{C}$  and at  $675^\circ\text{C}$ , the doping level increases with increasing Sb flux.

In order to analyze these results, we will consider that the temperature is sufficiently high and the growth rate sufficiently low in our experimental conditions to allow the *local equilibrium* regime to be achieved. This means that the surface coverage  $c_0$  is mainly driven by the balance between the incoming and desorbing Sb fluxes, while the doping level  $c_b$  accommodates the surface coverage under the constraint of Eq. (14). It is then possible to determine what are the coverages needed to reproduce the temperature dependence of the doping levels illustrated in Fig. 5. This only requires the knowledge of the segregation isotherms given by Eq. (14) at the

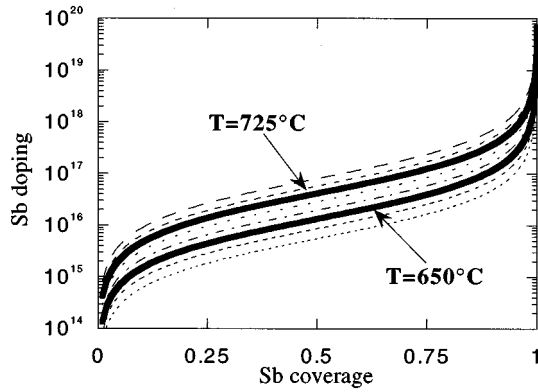


FIG. 6. Segregation isotherms for the Si(Sb) system ( $E_0^{\text{seg}} = -1.2$  eV) in the range of experimental temperatures:  $600^\circ\text{C} < T < 775^\circ\text{C}$ . The thick lines correspond to two temperatures characteristic of the two ( $T, F_{\text{Sb}}$ ) regimes (Fig. 1; Fig. 2).

experimental temperatures. One has then to determine the segregation energy  $E_0^{\text{seg}}$ , which can be done by fitting, using Eq. (14), the experimental variation of either the doping profile with surface coverage as reported by Delage *et al.*<sup>8</sup> at  $760^\circ\text{C}$ , or the segregation coefficient ( $r^{\text{Sb}} = c_0/c_b$ ) with temperature in a range for which segregation equilibrium is achieved as proposed by Barnett and Greene.<sup>10</sup> This leads to almost the same value for this segregation energy,  $E_0^{\text{seg}} = -1.2$  eV, which is very strong as expected from the synergy between the three driving forces of surface segregation for the Si(Sb) system. The segregation isotherms corresponding to the experimental temperatures are plotted in Fig. 6. As can be seen, they all exhibit the same trend, namely, the  $c_b(c_0)$  isotherms are of the Fowler-Guggenheim type with a large plateau (around  $c_b = 10^{-15} - 10^{-16}$  at/cm<sup>3</sup> in the low temperature regime and around  $c_b = 10^{-16} - 10^{-17}$  at/cm<sup>3</sup> in the higher one) for coverages  $0.2 < c_0 < 0.8$ , and then a sharp step rise for coverages  $0.8 < c_0 < 1$ . This shape is the signature of the existence, at lower temperature, of a first order phase transition between a Si-rich surface phase and a Sb-rich one. Let us now use these isotherms to interpret our experimental results for both substrates. This is done in Fig. 7 in which we have changed the ( $c_b, T$ ) map of Fig. 5 into a ( $c_0, T$ ) one, by using the relation  $c_0(c_b)$  displayed by the isotherms of Fig. 6. The main information given by Fig. 7 is that the Sb coverage (i) increases (as it should) when the temperature decreases for each substrate, (ii) is quasi-identical at a given temperature for the vicinal and nominal substrates in the low temperature regime [ $600^\circ\text{C} - 675^\circ\text{C}$ ], (iii) is lower by about 20% at a given temperature for the vicinal than for the nominal substrate in the higher temperature regime [ $700^\circ\text{C} - 775^\circ\text{C}$ ].

Therefore, our experimental Sb incorporation behavior should be completely understood from the coupling between desorption and segregation processes, provided that Sb desorption can be considered as identical for both nominal and vicinal substrates below  $700^\circ\text{C}$  but larger for the latter between  $700^\circ\text{C}$  and  $775^\circ\text{C}$ , leading to a Sb coverage lower by 20%. It is tempting to relate this proportion to that of step sites on the vicinal surface since, for a  $10^\circ$  misorientation, about 20% of surface sites are step ones. Therefore, our interpretation requires the desorption to occur essentially from

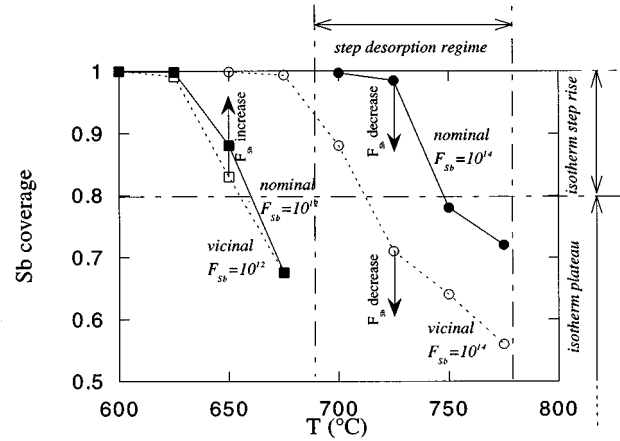


FIG. 7. Temperature dependence of the Sb coverage derived from Fig. 5 by assuming a local equilibrium driven by the surface segregation isotherms of Fig. 6.

step sites in the temperature range [ $700^\circ\text{C} - 775^\circ\text{C}$ ]. This is indeed what we have found in our previous thermodesorption studies on such misoriented surfaces,<sup>4</sup> which exhibited desorption peaks at lower temperature for vicinal than for nominal surfaces. The terrace peak was located at  $760 \pm 15^\circ\text{C}$ , whereas the peaks associated to steps were found at  $580 \pm 15^\circ\text{C}$  and  $675 \pm 15^\circ\text{C}$ , which corresponds exactly to the temperature range which is needed to interpret our incorporation data.

Let us just mention that, although the doping levels are indeed found almost equal for both substrates in the low temperature series, the doping profiles are less distorted for the vicinal than for the nominal one. This can be understood if one assumes that at low temperature, exchanges on the nominal surface are no longer instantaneous in which case the segregation regime is not at complete equilibrium. On the contrary, the vicinal surface presents steps which are preferential sites for exchange.<sup>17</sup> The energetic barrier is then lower so that there must exist a temperature range for which the misoriented surface is in a segregation equilibrium regime, whereas the nominal one is still limited by kinetics.

## VII. INFLUENCE OF THE Sb FLUX

The main conclusion of the preceding section is that there exists two different ranges: (i) for the Sb coverage  $c_0$ : [ $0.2 - 0.8$ ] where the doping level is almost constant and [ $0.8 - 1$ ] where it abruptly increases, due to the shape of the segregation isotherm; (ii) for the temperature  $T$ : [ $600^\circ\text{C} - 675^\circ\text{C}$ ] where the Sb coverage is the same for both substrates and [ $700^\circ\text{C} - 775^\circ\text{C}$ ] where it is lower for the vicinal substrate, due to desorption from steps (which will be referred to as the *step desorption regime*).

In order to check this conclusion, it was tempting to vary the incoming Sb flux for two temperatures chosen on both sides of  $700^\circ\text{C}$ . We have then chosen  $650^\circ\text{C}$  and  $725^\circ\text{C}$  for which, according to Fig. 7, different behaviors should be observed. Indeed, in the former case ( $T = 650^\circ\text{C}$ ) one can see that varying the flux (see arrow in Fig. 7) allows the coverage to vary, similarly for both substrates, in a region

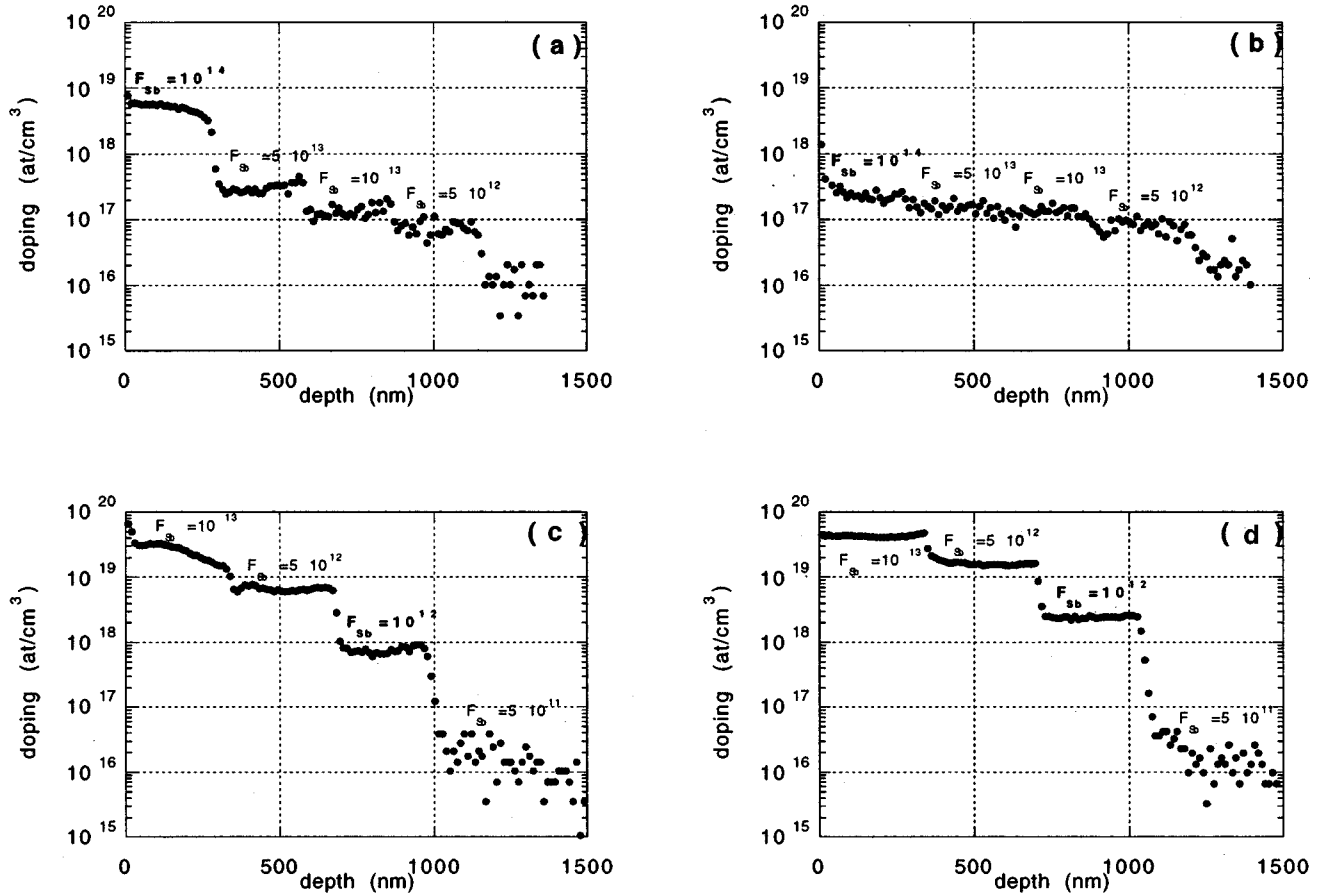


FIG. 8. Flux dependence of the doping profile for two temperatures,  $T=725\text{ °C}$  (a-b) and  $T=650\text{ °C}$  (c-d), and two misorientation angles,  $\alpha=0\text{ °}$  (a-c) and  $\alpha=10\text{ °}$  (b-d). The flux units are  $\text{at}/(\text{cm}^2\text{ s})$ .

limited to the  $[0.8-1]$  coverage corresponding to the isotherm step rise. Therefore one expects the doping level to increase with the flux in the same way in both cases. On the contrary in the latter case ( $T=725\text{ °C}$ ), one can see that, due to the lower coverage for the vicinal surface, varying the flux gives access again to the  $[0.8-1]$  coverage region (isotherm step rise) for the nominal substrate but to the other region  $[0.5-0.8]$ , corresponding to the isotherm plateau, for the vicinal one. As a consequence, one should observe in that case a decrease of the doping profile with decreasing flux for the nominal surface but almost no evolution for the vicinal one.

We have then varied experimentally the Sb flux at these two temperatures for both the nominal and vicinal substrates, which led to the doping profiles illustrated in Fig. 8. As can be seen, the main trends completely confirm our predictions. Indeed, the doping level obviously increases with increasing Sb flux (and then with surface coverage) but one observes drastic differences between the two temperature regimes. In the higher one ( $T=725\text{ °C}$ ), this increase is only observed for the nominal surface, the doping level remaining quasi-constant (as expected) for the misoriented one. In the lower one ( $T=650\text{ °C}$ ), one can see that the difference between

both orientations is strongly reduced, confirming that in this case the step desorption is no longer active.

## VIII. CONCLUSION

From this study one can conclude that the Sb doping incorporation presents qualitatively similar variations with temperature for vicinal and nominal Si(111) substrates, namely no variation above a temperature  $T_c$  and then an abrupt increase below. Only the value of  $T_c$  depends on the surface misorientation, which has to be related to the coupled effects of desorption and segregation processes. More precisely, the lower value found for  $T_c$  in the case of the vicinal substrate is due to the existence of an intermediate temperature range  $[700\text{ °C}-775\text{ °C}]$  for which Sb atoms essentially desorb from steps, which is in full agreement with previous thermodesorption experiments.<sup>4</sup> Therefore, for temperatures above  $700\text{ °C}$  the doping level is weaker for the misoriented than for the nominal sample whereas below it is the same in both cases.

## ACKNOWLEDGMENT

The CRMC2 is also associated to the Universities of Aix-Marseille II and III.

- <sup>1</sup>E. Rosencher, S. Delage, Y. Campidelli, and F. Arnaud d'Avitaya, *Electron. Lett.* **20**, 762 (1984).
- <sup>2</sup>H. Kibbel and E. Kasper, *Vacuum* **41**, 929 (1990).
- <sup>3</sup>M. Ladevèze, I. Berbezier, and F. Arnaud d'Avitaya, *Surf. Sci.* **352-54**, 797 (1996).
- <sup>4</sup>M. Ladevèze, G. Trégliia, P. Muller, and F. Arnaud d'Avitaya, *Surf. Sci.* (to be published).
- <sup>5</sup>J. C. Bean, *Appl. Phys. Lett.* **33**, 654 (1978).
- <sup>6</sup>U. Konig, E. Kasper, and H. J. Herzog, *J. Cryst. Growth* **52**, 151 (1981).
- <sup>7</sup>R. A. Metzger and F. G. Allen, *J. Appl. Phys.* **55**, 931 (1984).
- <sup>8</sup>S. Delage, Y. Campidelli, F. Arnaud d'Avitaya, and S. Tatarenko, *J. Appl. Phys.* **61**, 1404 (1987).
- <sup>9</sup>S. S. Iyer, R. A. Metzger, and F. G. Allen, *J. Appl. Phys.* **52**, 5608 (1981).
- <sup>10</sup>S. A. Barnett and J. E. Greene, *Surf. Sci.* **151**, 67 (1985).
- <sup>11</sup>H. Jorke, *Surf. Sci.* **193**, 569 (1988).
- <sup>12</sup>F. Ducastelle, B. Legrand, and G. Trégliia, *Prog. Theor. Phys. Suppl.* **101**, 159 (1990).
- <sup>13</sup>A. Senhaji, G. Trégliia, B. Legrand, N. T. Barrett, C. Guillot, and B. Vilette, *Surf. Sci.* **274**, 297 (1992).
- <sup>14</sup>M. Lagues and J. L. Domange, *Surf. Sci.* **47**, 77 (1975).
- <sup>15</sup>J. M. Moison, C. Guille, F. Houzay, F. Barthe, and M. Van Rompay, *Phys. Rev. B* **40**, 6149 (1989).
- <sup>16</sup>J. Nagle, J. P. Landesman, M. Larive, C. Mottet, and P. Bois, *J. Cryst. Growth* **127**, 550 (1993).
- <sup>17</sup>H. Ibach, M. Giesen, T. Flores, M. Wuttig, and G. Trégliia, *Surf. Sci.* **364**, 453 (1996).